

# Fast Semantic Segmentation of RGB-D Scenes with GPU-Accelerated Deep Neural Networks

Nico Höft, Hannes Schulz, and Sven Behnke

Rheinische Friedrich-Wilhelms-Universität Bonn  
Institut für Informatik VI, Friedrich-Ebert-Allee 144  
{hoeft@cs, schulz@ais, behnke@cs}.uni-bonn.de

**Abstract.** In semantic scene segmentation, every pixel of an image is assigned a category label. This task can be made easier by incorporating depth information, which structured light sensors provide. Depth, however, has very different properties from RGB image channels. In this paper, we present a novel method to provide depth information to convolutional neural networks. For this purpose, we apply a simplified version of the histogram of oriented depth (HOD) descriptor to the depth channel. We evaluate the network on the challenging NYU Depth V2 dataset and show that with our method, we can reach competitive performance at a high frame rate.

**Keywords:** deep learning, neural networks, object-class segmentation

## 1 Introduction

Semantic scene segmentation is a major challenge on the way to functional computer vision systems. The task is to label every pixel in an image with surface category it belongs to. Modern depth cameras can make the task easier, but the depth information needs to be incorporated into existing techniques. In this paper, we demonstrate how depth images can be used in a convolutional neural network for scene labeling by employing a simplified version of the histogram of oriented gradients (HOG) descriptor to the depth channel (HOD). We train and evaluate our model on the challenging NYU Depth dataset and compare its classification performance and execution time to state of the art methods.

## 2 Network Architecture

We train a four-stage convolutional neural network, which is illustrated in Fig. 1, for object-class segmentation. The network structure, proposed by Schulz and Behnke [1], is derived from traditional convolutional neural networks, but has inputs at multiple scales. In contrast to classification networks, there are no fully connected layers at the top—the output maps are also convolutional.

The first three stages  $s = \{0, 1, 2\}$  have input, hidden convolutional, and output maps  $I_s, C_s, O_s$ , respectively. Pooling layers  $P_s, P'_s$  between the stages

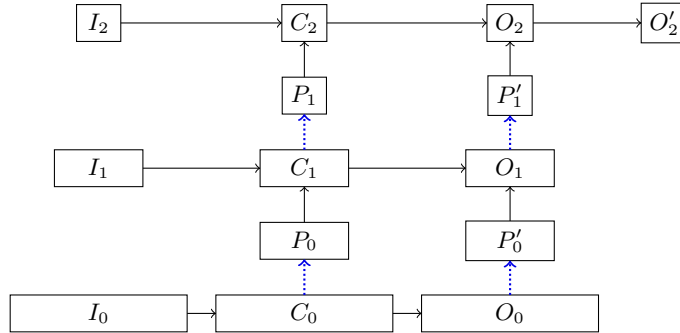


**Fig. 1.** Network structure used in this paper. On stage  $s$ ,  $I_s$  is input,  $C_s$  a convolution,  $O_s$  the output, and  $P_i$  a pooling layer. Outputs of stage  $s$  are refined in stage  $s + 1$ , final outputs are refined from  $O_2$  to  $O'_2$ . Solid and dashed arrows denote convolution and max-pooling operations, respectively. Every stage corresponds to a scale at which inputs are provided and outputs are evaluated.

reduce the resolution of the map representations. The output layer  $O'_2$  is the last stage. The network differs from common deep neural networks, as it is trained in stage-wise supervised manner and the outputs of the previous stage are supplied to the next stage to be refined. Thus, the lower stages provide a prior for the higher stages, while the simultaneous subsampling allows for the incorporation of a large receptive field into the final decision.

Every layer consists of multiple maps. Input layers have three maps for ZCA-whitened RGB channels, as well as five maps for histograms of oriented gradients and depth each (detailed in Section 4). Intermediate layers contain 32 maps. Convolutions extract local features from their source maps. Following Schulz and Behnke [1], all convolution filters have a size of  $7 \times 7$ , except for the last filter. The last filter has a size of  $11 \times 11$  and only re-weights previous classification results, taking into account a larger receptive field. Also note that there are no fully connected layers—the convolutional output layers have one map for every class, and a pixel-wise multinomial logistic regression loss is applied. In contrast to Schulz and Behnke [1], we use rectifying non-linearities  $\sigma(x) = \max(x, 0)$  after convolutions. This non-linearity improves convergence [2] and results in more defined boundaries in the output maps than sigmoid non-linearities. When multiple convolutions converge to a map, their results are added before applying a non-linearity.

### 3 Related Work

Our work builds on the architecture proposed in Schulz and Behnke [1], which (in the same year as Farabet et al. [3]) introduced neural networks for RGB scene segmentation. We improve on their model by employing rectifying non-linearities, recent learning algorithms, online pre-processing, and providing depth information to the model.

Scene labeling using RGB-D data was introduced with the NYU Depth V1 dataset by Silberman and Fergus [4]. They present a CRF-based approach and provide handcrafted unary and pairwise potentials encoding spatial location and relative depth, respectively. These features improve significantly over the depth-free approach. In contrast to their work, we use learned filters to combine predictions. Furthermore, our pipeline is less complex and achieves a high framerate. Later work [5] extends the dataset to version two, which we use here. Here, the authors also incorporate additional domain knowledge into their approach, which further adds to the complexity.

Couprie et al. [6] present a neural network for scene labeling which is very close to ours. Their network processes the input at three different resolutions using the same network structure for each scale. The results are then upsampled to the original size and merged within superpixels. Our model is only applied once to the whole image, but uses inputs from multiple scales, which involves less convolutions and is therefore faster. Outputs are also produced at all scales, but instead of a heuristic combination method, our network learns how to use them to improve the final segmentation results. Finally, the authors use raw depth as input to the network, which cannot be exploited easily by a convolutional neural network, e.g., absolute depth is less indicative of object boundaries than are relative depth changes.

A common method for pixel-wise labeling are random forests [7, 8], which currently provide the best results for RGB-D data [9, 10]. These methods scale feature size to match the depth for every image position. Our convolutional network does not normalize the feature computation by depth, which makes it easy to reuse lower-level features for multiple higher-level computations.

## 4 Pre-Processing

Since our convolution routines<sup>1</sup> only support square input images, we first extend the images with mirrored margins. To increase generalization, we generate variations of the training set. This is performed online on the CPU while the GPU evaluates the loss and the gradient, at no cost of speed. We randomly flip the image horizontally, scale it by up to  $\pm 10\%$ , shift it by up to seven pixels in horizontal and vertical direction and rotate by up to  $\pm 5^\circ$ . The depth channel is processed in the same way. We then generate three types of input maps.

From random patches in the training set, we determine a whitening filter that decorrelates RGB channels as well as neighboring pixels. Subtracting the mean and applying the filter to an image yields three zero phase (ZCA) whitened image channels.

On the RGB-image as well as on the depth channel, we compute a computationally inexpensive version of histograms of oriented gradients (HOG [11]) and histogram of oriented depth (HOD [12]) as follows.

For every pixel  $p$ , we determine its gradient direction  $\alpha_p$  and magnitude  $n_p$ . The absolute value of  $|\alpha_p|$  is then quantized by linear interpolation into two of five bins at every image location, and weighted by  $n_p$ . To produce histograms of

<sup>1</sup> We employ convolutions from the cuda-convnet framework of Alex Krizhevsky.

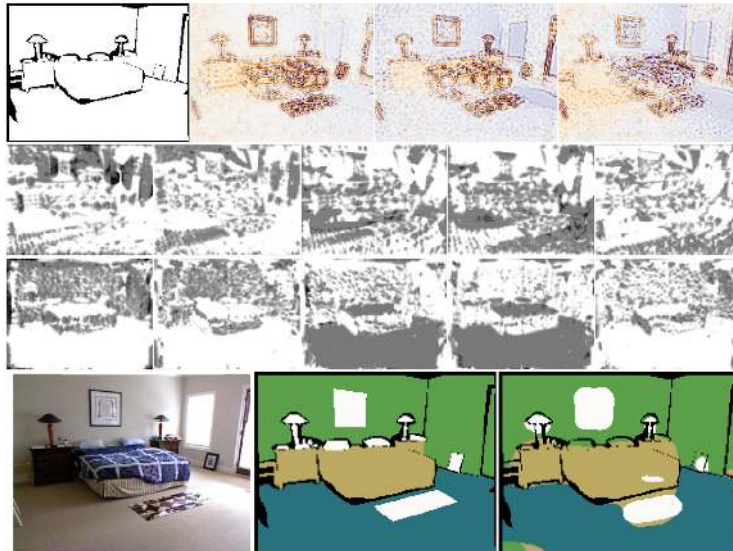


Fig. 2. Network maps, inputs and outputs. First row, ignore mask and ZCA-whitened RGB channels. Second and third row, HOG and HOD maps, respectively. Fourth row, original image, ground truth and network prediction multiplied by ignore mask for reference. Mirrored margins are removed for presentation to save space. Note that HOG and HOD encode very different image properties with similar statistics.

the orientation strengths present at all locations, we apply a Gaussian blur filter to all quantization images separately. Finally, the histograms are normalized with the  $L_2$ -norm.

The main difference to the standard HOG descriptor is that no image *cells* are combined into a single descriptor. This leaves it to the network to incorporate long-range dependencies and saves space, since our descriptor contains only five values per pixel.

All maps are normalized to have zero mean and unit variance over the training set. The process is repeated for every scale, where the size is reduced by a factor of two. For the first scale, we use a size of  $196 \times 196$ . The teacher maps are generated from ground truth by downsampling, rotating, scaling, and shifting to match the network output. We use an additional ignore map, which sets the loss to zero for pixels which were not annotated or where we added a margin to the image by mirroring. Sample maps and segmentations are shown in Fig. 2.

## 5 Experiments

We split the training data set into 796 training and 73 validation images. In a stage  $s$ , we use the RMSProp learning algorithm with an initial learnrate  $10^{-4}$ , to train the weights of all stages below or equal to  $s$ . The active stage is automatically switched once the validation error increases or fails to improve. The pixel mean of the classification error over training is shown in Fig. 3. During the first two stages, training and validation error behave similarly, while in the final

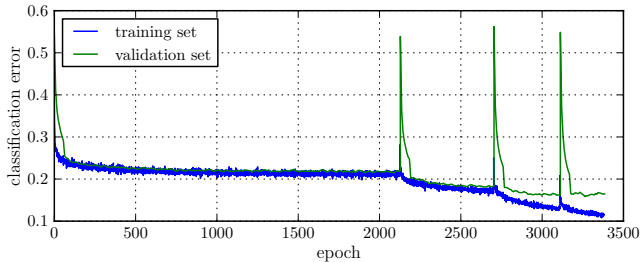


**Fig. 3.** Classification error on NYU Depth V2 during training, measured as the mean over output pixels. The peaks and subsequent drops occur when one stage is finished and learning proceeds to the next—randomly initialized—stage.

**Table 1.** Classification Results on NYU Depth V2

Method	Floor	Structure	Furniture	Props	Pixel Acc.	Class Acc.
Ours without depth	69.1	57.8	55.7	41.7	56.2	56.1
Ours with depth	77.9	65.4	<b>55.9</b>	<b>49.9</b>	61.1	62.0
[6] without depth	68.1	<b>87.8</b>	51.1	29.9	59.2	63.0
[6] with depth	<b>87.3</b>	86.1	45.3	35.5	63.5	64.5

stages the network capacity is large enough to overfit.

*Classification Performance.* To evaluate performance on the 580 image test set, we crop the introduced margins, determine the pixel-wise maximum over output maps and scale the prediction to match the size of the original image. There are two common error metrics in the literature, the average pixel accuracy and the average accuracy over classes, both of which are shown in Table 1. Our network benefits greatly from the introduction of depth maps, as apparent in the class accuracy increase from 56.1 to 62.0. We compare our results with the architecture of Couprie et al. [6], which is similar but computationally more expensive. While we do not reach their overall accuracy, we outperform their model in two of the four classes, *furniture* and, interestingly, the rather small *props*—despite our coarser output resolution.

*Prediction Speed.* We can also attempt to compare the time it takes to process an image by the network. Couprie et al. [6] report 0.7s per image on a laptop. We process multiple images in parallel on a GPU. With asynchronous pre-processing, our performance saturates at a batch size of 64, where we are able to process 52 frames per second on a 12 core Intel Xeon at 2.6GHz and a NVIDIA GeForce GTX TITAN GPU. Note that this is faster than the frame rate of the sensor collecting the dataset (30Hz). While the implementation of Couprie et al. [6] could certainly also profit from a GPU implementation, it requires more convolutions as well as expensive superpixel averaging and upscaling operations. Our network is also faster than random forests on the same task (30.3fps [10], hardware similar to ours).

## 6 Conclusion

We presented a convolutional neural network architecture for RGB-D semantic scene segmentation, where the depth channel is provided as feature maps representing components of a simplified histogram of oriented depth (HOD) operator. We evaluated the network on the challenging NYU Depth V2 dataset and found that introducing depth significantly improved the performance of our model, resulting in competitive classification performance. In contrast to other published results of neural network and random-forest based methods, our GPU implementation is able to process images at a high framerate of 52 fps.

## References

- [1] H Schulz and S Behnke. “Learning object-class segmentation with convolutional neural networks”. In: *Eur. Symp. on Art. Neural Networks*. 2012.
- [2] A Krizhevsky, I Sutskever, and G Hinton. “Imagenet classification with deep convolutional neural networks”. In: *Adv. in Neural Information Processing Systems*. 2012.
- [3] C Farabet, C Couprie, L Najman, and Y LeCun. “Scene parsing with multiscale feature learning, purity trees, and optimal covers”. In: *arXiv preprint arXiv:1202.2160* (2012).
- [4] N Silberman and R Fergus. “Indoor scene segmentation using a structured light sensor”. In: *Int. Conf. on Computer Vision (ICCV) Workshops*. 2011.
- [5] N Silberman, D Hoiem, P Kohli, and R Fergus. “Indoor Segmentation and Support Inference from RGBD Images”. In: *Europ. Conf. on Computer Vision (ECCV)*. 2012.
- [6] C Couprie, C Farabet, L Najman, and Y LeCun. “Indoor Semantic Segmentation using depth information”. In: *CoRR* abs/1301.3572 (2013).
- [7] T Sharp. “Implementing decision trees and forests on a GPU”. In: *Europ. Conf. on Computer Vision (ECCV)*. 2008.
- [8] J Shotton, T Sharp, A Kipman, A Fitzgibbon, M Finocchio, A Blake, M Cook, and R Moore. “Real-time human pose recognition in parts from single depth images”. In: *Communications of the ACM* (2013).
- [9] J Stückler, B Waldvogel, H Schulz, and S Behnke. “Dense real-time mapping of object-class semantics from RGB-D video”. In: *Journal of Real-Time Image Processing* (2013).
- [10] AC Müller and S Behnke. “Learning Depth-Sensitive Conditional Random Fields for Semantic Segmentation of RGB-D Images”. In: *Int. Conf. on Robotics and Automation (ICRA)*. 2014.
- [11] N Dalal and B Triggs. “Histograms of oriented gradients for human detection”. In: *Computer Vision and Pattern Recognition (CVPR)*. 2005.
- [12] L Spinello and KO Arras. “People detection in RGB-D data”. In: *Int. Conf. on Intelligent Robots and Systems (IROS)*. IEEE. 2011.